J Neurophysiol
88: 2088–2095, 2002; 10.1152/jn.00860.2001.

Localizing Visual Discrimination Processes in Time and Space

JENS-MAX HOPF,[1] EDWARD VOGEL,[2] GEOFFREY WOODMAN,[3] HANS-JOCHEN HEINZE,[1] AND STEVEN J. LUCK[3]

[1]*Department of Neurology II, Otto-von-Guericke University, D-39120 Magdeburg, Germany;* [2]*Department of Psychology, University of Oregon, Eugene, Oregon 97403-1227; and* [3]*Department of Psychology, University of Iowa, Iowa City, Iowa 52242-1407*

Received 18 October 2001; accepted in final form 10 June 2002

Hopf, Jens-Max, Edward Vogel, Geoffrey Woodman, Hans-Jochen Heinze, and Steven J. Luck. Localizing visual discrimination processes in time and space. *J Neurophysiol* 88: 2088–2095, 2002; 10.1152/jn.00860.2001. Previous studies of visual processing in humans using event-related potentials (ERPs) have demonstrated that task-related modulations of an early component called the "N1" wave (140–200 ms) reflect the operation of a voluntary discrimination process. Specifically, this component is larger in tasks requiring target discrimination than in tasks requiring simple detection. The present study was designed to localize this discriminative process in both time and space by means of combined magnetoencephalographic (MEG) and ERP recordings. Discriminative processing led to differential ERP and MEG activity beginning within 150 ms of stimulus onset. Source localization of the combined ERP/MEG data was performed using anatomical constraints from structural magnetic resonance images. These analyses revealed highly reliable and focused activity in regions of inferior occipital-temporal cortex. These findings indicate that the earliest measurable correlates of discriminative operations in the visual system appear as neural activity in circumscribed regions of the ventral processing stream.

INTRODUCTION

The initial processing of visual stimuli appears to be entirely automatic, occurring regardless of task demands. For example, neural activity in the retina appears to be insensitive to the direction of covert attention (Mangun et al. 1986). Once visual information reaches primary visual cortex (area V1), factors such as arousal and spatial attention can influence neural activity (Gandhi et al. 1999; Ito and Gilbert 1999; Motter 1993; Roelfsema et al. 1998; Shulman et al. 1997; Somers et al. 1999). However, the effects of top-down factors are smaller in area V1 than in extrastriate visual areas (Kastner et al. 1998; Tootell et al. 1998), and these effects may reflect feedback rather than a modulation of the initial feedforward volley of sensory activity (Clark and Hillyard 1996; Martinez et al. 1999; Roelfsema et al. 1998). In contrast, top-down modulations of activity in extrastriate and inferotemporal visual areas are quite robust, and at least some extrastriate attention effects reflect a modulation of feedforward sensory activity (Hillyard et al. 1998; Luck et al. 1997; Mangun et al. 1997). In general, top-down factors play an increasing role as visual information reaches higher levels of processing, defined both in terms of neuroanatomy (i.e., larger top-down effects in higher-level cortical regions) and time (i.e., top-down effects become larger as more time elapses after stimulus onset).

The intention to make a visual discrimination can also influence neural responses. For example, Spitzer and Richmond (1991) found that stimulus-elicited responses in macaque inferotemporal neurons were smallest when the stimuli were task-irrelevant, became larger when the monkeys were required to make a simple detection response, and were largest when the monkeys were required to make a discriminative response. The time course of these effects was not analyzed, but the effects appeared to begin within 150 ms of stimulus onset.

The effects of discriminative processing have also been examined in neuroimaging studies that were focused on attention, but manipulated attention by varying the type of discrimination performed by the subjects. For example, Corbetta et al. (1990, 1991) found that blood flow was increased in different regions of visual cortex when subjects discriminated color, form, and velocity. Similarly, Clark et al. (1997) found differential patterns of activation when subjects discriminated color versus face identity, and Wojciulik et al. (1998) found that activity in the fusiform face area was influenced by whether subjects performed a face-matching task or a house-matching task. In a recent PET study, Dupont et al. (1998) report activity in fusiform gyrus and other regions in a orientation-discrimination task using square-wave gratings. However, given the relatively poor temporal resolution of neuroimaging techniques, these effects might reflect preparatory processes or postperceptual processes rather than perceptual-discrimination processes.

The time course of discriminative processing has been studied with event-related potential (ERP) recordings. For example, Ritter and his colleagues have conducted several experiments comparing two tasks, a *simple-response* task in which subjects made a speeded response as soon as they detected a stimulus, regardless of its form and a *discriminative-response* task in which subjects made different responses depending on the form of the stimulus (Ritter et al. 1982, 1983, 1988). The initial P1 sensory response was the same for these two conditions, but the subsequent N1 wave was larger in the discriminative-response condition than in the simple-response condi-

Address for reprint requests: J.-M. Hopf, Dept. of Neurology II, Otto-von-Guericke-University, D-39120 Magdeburg, Germany, Leipziger Str. 44, D-39120 Magdeburg, Germany (E-mail: jens-max.hopf@medizin.uni-magdeburg.de).

The costs of publication of this article were defrayed in part by the payment of page charges. The article must therefore be hereby marked "*advertisement*" in accordance with 18 U.S.C. Section 1734 solely to indicate this fact.

tion, beginning around 150 ms poststimulus. Ritter et al. (1982) concluded that this effect reflected the operation of a pattern discrimination process. More recently, Vogel and Luck (2000) found that this N1 discrimination effect can be found for color discriminations as well as for form discriminations and concluded that it reflects a more general discrimination process. Vogel and Luck also found that the N1 discrimination effect does not simply reflect increased arousal or increased perceptual load. Thus the intention to perform a discrimination can influence neural activity in the human brain within 150 ms of stimulus onset.

A similar N1 modulation has been found for attentional orienting in space (Luck and Hilyard 1995; Mangun 1995). That is, stimuli at attended locations elicit a larger N1 component than stimuli at unattended locations (we call this the N1 spatial attention effect). The time course and scalp topography of this N1 spatial attention effect resemble those of the N1 discrimination effect. Moreover, the N1 spatial attention effect appears to be present only when the attended stimulus necessitates some form of discriminative response (Mangun and Hillyard 1991). Hence the parallels between both N1 effects suggest that the N1 spatial attention effect may represent an ERP instantiation of the same discriminative operation under somewhat different experimental conditions.

The finding of similar ERP effects for manipulations of attention and manipulations of discrimination make it clear that it is sometimes difficult to distinguish between the concepts of attention and discrimination. This is a very complex issue that has been discussed in detail elsewhere (Luck and Vecera 2002). For the sake of simplicity, this article will make no distinction between discrimination processes per se and discrimination-related aspects of attention.

The purpose of the present study is to link the precise temporal information provided by human ERP recordings of the N1 discrimination effect with the underlying neuroanatomy. To accomplish this, we recorded both ERPs and MEG responses in simple- and discriminative-response conditions. We then subtracted the waveforms obtained in the simple-response condition from the waveforms obtained in the discriminative-response condition to isolate activity related to top-down control of discriminative processing. The neuroanatomical sources of this differential activity were then localized for each subject and for the grand average with the aid of structural magnetic resonance (MR) images of each subject's brain.

METHODS

Subjects

Ten subjects (mean age: 25.9 yr; 5 female; 1 left handed) with normal color vision and normal or corrected-to-normal visual acuity participated in this experiment. The experiment was undertaken with the understanding and written consent of the subjects. Subject were paid for participation.

Stimuli and procedure

The stimuli and procedure are illustrated in Fig. 1. Stimuli were back-projected from a video projector onto a screen at a viewing distance of 120 cm. The screen was gray (5.0 cd/m^2) and contained a continuously visible fixation point at the center. The imperative stimulus was a 2 × 2° square centered at the fixation point. Each square

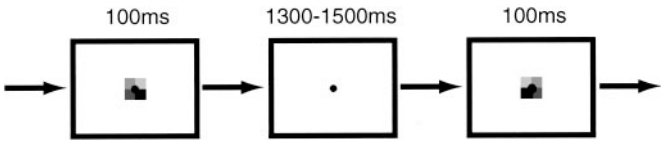

FIG. 1. Principial trial structure. While continuously fixating the the center dot, subjects were required to discriminate the presence or absence of the target color by alternative button presses (discriminative-response condition) or to press a button for each imperative stimulus, regardless of the presence or absence of the target color (simple-response condition).

was divided into four 1 × 1° quadrants, each filled with a different color selected from a set of six colors (red, green, blue, yellow, brown, pink; luminances between 53 and 78 cd/m^2). The colors of the quadrants were selected at random, without replacement, with the constraint that one of the quadrants was red (the target color) on 10% of trials.

Subjects performed simple- and discriminative-response tasks in separate blocks of trials. In the discriminative-response condition, subjects discriminated the presence of the red target color, pressing a button with one hand if red was present in the imperative stimulus and pressing a button with the opposite hand if the target was absent. The assignment of responses to hands was counterbalanced across subjects. In the simple-response condition, subjects were required to press a button for each imperative stimulus, regardless of the presence or absence of the target color. For each subject, the response hand used in the simple-response condition was the same as the response hand used on the red-absent trials in the discriminative-response condition. In both conditions, subjects were instructed to respond as quickly as possible without making errors.

Each stimulus was presented for 100 ms, with a stimulus onset asynchrony that varied randomly between 1,300 and 1,500 ms (rectangular distribution). On 10% of trials, the imperative stimulus was replaced by a 100-ms stimulus-free interval; subjects were instructed to make no response on these catch trials.

Subjects performed eight trial blocks in each condition, alternating between the simple- and discriminative-response conditions; half of the subjects started with the simple-response condition and half with the discriminative-response condition. Each block consisted of 300 trials, including 30 catch trials, 30 red-present trials, and 240 red-absent trials. Thus each subject received a total of 1,920 target-absent trials; this very large number of trials was intended to yield a high signal-to-noise ratio.

Recording and analysis

The MEG and electroencephalographic (EEG) signals were recorded simultaneously using a BTi Magnes 2500 whole-head MEG system (Biomagnetic Technologies) with 148 magnetometers for the MEG and an electrode cap (Electrocap International) in conjunction with a 32-channel Synamps amplifier (NeuroScan) for the EEG. Electrode locations were chosen according to standard electrode montage of the American Electroencephalographic Society (1994) (Fpz, Fz, Cz, Pz, Oz, Iz, Fp1, Fp2, F7, F8, F3, F4, FC1, FC2, T7, T8, C3, C4, CP1, CP2, P7, P8, P3, P4, PO3, PO4, PO7, PO8, IN3, IN4). High resolution anatomical MR scans (GE Signa Horizon LX 1.5 T Neuro-optimized MR) were acquired during a separate session using a quadrature head coil [3-dimensional (3D) spoiled gradient echo sequence, TR 24 ms, TE 8 ms, flip angle 24°, voxel size 1 × 1 × 1.5 mm, matrix dimensions 256 × 256 × 124].

The MEG and EEG signals were filtered with a band-pass of DC–50 Hz and digitized with a sampling rate of 254 Hz. The MEG was also subjected to an on-line noise reduction process that removes a weighted sum of environmentally induced magnetic noise measures (first-order spatial gradients of the field) recorded by eight remote reference channels that do not pick up brain activity (Robinson 1989). Artifact rejection was performed off-line by discarding epochs with

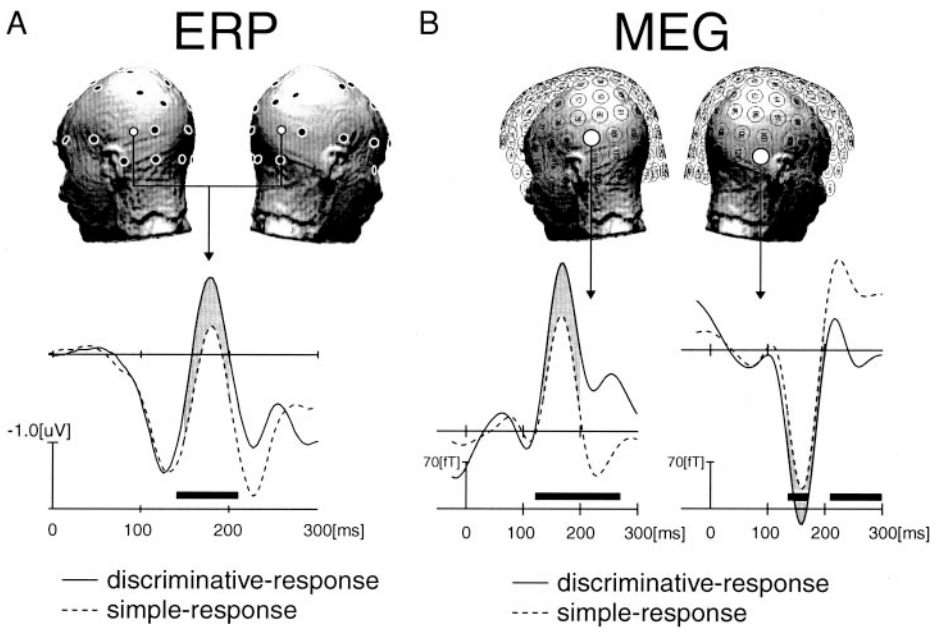

FIG. 2. *A*: grand-average event-related potentials (ERP) waveforms for nontarget stimuli in the simple- and discriminative-response condition at scalp locations showing the maximum discriminative-simple difference. The gray area between waveforms indicates the time range of the N1 component. The shown waveforms were recorded from left (PO7) and right (PO8) occipital electrode sites (white circles) and averaged across hemispheres. The black horizontal bar at the abszissa indicates the time range of significant differences ($P < 0.05$). *B*: grand-average MEG waveforms from 2 posterior sensor sites (white circles). The gray area between waveforms indicates the time range of the magnetic analog of the N1 component. The black horizontal bars at the abszissa indicate time ranges of significant differences ($P < 0.05$).

peak-to-peak amplitudes exceeding a threshold of 3.0×10^{-12} T for the MEG and 100 μV for the EEG.

For each subject, a Polhemus 3Space Fastrak system was used to measure the 3D of the EEG electrodes and three skull/scalp landmarks (nasion and left and right preauricular points). The locations of these landmarks in relation to the MEG sensor positions were derived on the basis of localization signals provided by five spatially distributed coils attached to the subject's head with a fixed spatial relation to the landmarks. These landmarks, in turn, were matched with the individual subjects' anatomical MR scans.

Analyses were performed on both individual subjects and on a grand average across all subjects. To compute the grand average activity, the coordinate system for each subject was readjusted to the coordinate system of one reference subject, whose anatomical MR scan was used for the grand-average source analyses. This MR scan was, in turn, spatially normalized into the standardized reference frame of Talairach and Tournoux (1988) for the purpose of reporting MEG source localization coordinates.[1]

Average waveforms for both MEG and EEG were computed for each subject, time-locked to stimulus onset, with a100-ms prestimulus baseline interval. Separate averages were derived for the discriminative- and simple-response conditions. Averages were computed only for imperative stimuli lacking the red target color; the electrophysiological data from target-present stimuli and catch trials will not be considered in this report. The N1 discrimination effect was isolated by computing difference waves in which simple-response waveforms were subtracted from discriminative-response waveforms (these are called the discriminative–simple difference waveforms). This effect was quantified as the mean amplitude in these difference waveforms between 140 and 200 ms, relative to the 100-ms prestimulus baseline. Statistical analyses were performed with repeated-measures ANOVAs, using the Greenhouse-Geisser epsilon correction for nonsphericity when appropriate (Jennings and Wood 1976).

For each subject, source analysis was performed on the discriminative–simple difference waveforms using the multi-modal neuroimaging software Curry 4.0 (Philips Electronics N.V.). For source reconstruction, the MEG and ERP data were combined in a general model to achieve maximum localization power (Fuchs et al. 1998b). Realistic 3D-volume conductor models for each subject were derived by segmenting the individual MR scans into three shells (cortical surface, cerebrospinal fluid space, and bone structure of the scull) using the boundary element method (BEM) (Fuchs et al. 1998a). A distributed source model (a model of the distribution of current over the cortical surface) served for source localization based on the minimum norm least-squares method (MNLS) (Fuchs et al. 1999). In this model, the BEM surface grid of the cortical surface was used as a predefined source compartment. Inherent in the MNLS model is the natural bias toward high gain source locations that would overemphasize superficial source locations. This was compensated by an additional model term that weights the estimated currents to account for the lower gains of deeper dipole components (cf. Curry User Guide, Philips Electronics N.V. p. 151–154). Finally, the regularization parameter that links the model term to the data were determined by the χ^2 criterion relying on the assumption that the data misfit is in the order of the amount of noise in the data. Noise was estimated from baseline magnetic activity within a period of 100 ms preceding stimulus onset.

The same approach to source reconstruction was applied to the grand average MEG and ERP data using the BEM model of the reference subject (*subject 8*).

RESULTS

Electrical waveforms and distributions

Figure 2*A* shows the grand-average ERP waveforms for nontarget stimuli in the simple-response and discriminative-response conditions. The waveforms shown in this figure were recorded from parietal-occipital sites (PO7 and PO8, white circles), averaged across hemispheres. The gray area illustrates the N1-discrimination effect, which consists of greater negativity in the discriminative-response condition relative to the

[1] The following steps were applied to transform the cortical surface of individual brains into the reference space of Talairach and Tournoux (1988). *1*) The individual brain was first roughly centered into the Talairach-space using the extensions of the subject's brain on the principal axes (*x, y, z*) of the Talairach AC/PC-based system. *2*) (*x-y-z*) extensions of 260 equidistantly spaced locators were then obtained from the surface-envelope of the reference brain of Talairach and Tournoux (1988) (Data from all 3 slice-orientations were taken into account). *3*) The extensions of an equivalent set of 260 locators were obtained from the surface of the individual brain. *4*) The deviation between corresponding sets of locators was minimized by deforming the subject's individual cortex surface using linear scaling and rotation in 3 principal directions (for rotation, additional locators in the gap between the hemispheres were also used).

simple-response condition. This effect began at approximately 140 ms and continued until approximately 270 ms. Ritter et al. (1982, 1983) argued that this effect consists of an early phase and a late phase and demonstrated that only the early phase corresponds to discriminative processing per se. The late phase, in contrast, was shown to reflect subsequent processing stages that are more related to stimulus classification and target probability. Moreover, changing discrimination difficulty modulated the later but not the early phase (Ritter et al. 1988). A functional separation into early and late phases was furthermore suggested by differences in scalp topography. In particular, the scalp topography of the later phase differed for physical and semantic discrimination tasks. Hence, the later phase seems to reflect heterogeneous aspects of stimulus processing that go far beyond elementary discriminative processes. Because this report investigates the neural sources underlying earliest discriminative processing, we will focus exclusively on the early phase (140–200 ms), which is indicated by the gray region in Fig. 2*A*.

Figure 3*A* shows the time course the discriminative-simple difference along with the scalp distribution of the early phase (140–200 ms). This effect had a broad occipital distribution with a larger amplitude over the left hemisphere.

A repeated-measures ANOVA was performed on the N1 measurements for the simple- and discriminative-response conditions. Three factors were included: condition, anterior-posterior electrode position, and electrode hemisphere (the midline electrode sites were excluded). The larger N1 observed for the discriminative-response condition yielded a significant main effect of condition ($F(1,9) = 11.93$, $P < 0.005$). The occipital maximum of this effect yielded a significant 2-way interaction between condition and anterior-posterior electrode position ($F(1,9) = 13.8$, $P < 0.005$).

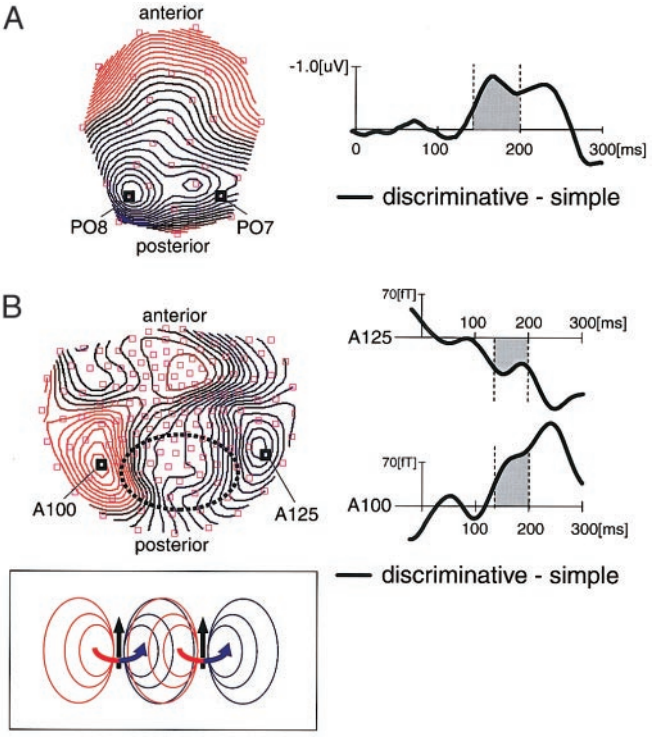

FIG. 3. *A*: grand-average ERP scalp distribution of the discriminative-simple difference waveform in the time range of the N1 wave. The difference waveform (*right*) was recorded from 2 posterior electrode sites (PO7/PO8) and averaged across hemipheres. The gray area indicates the time range for which the scalp distribution was computed. *B*: grand-average magnetic field distribution of the discriminative-simple difference waveform in the time range of the magnetic analog of the N1 component. The difference waveforms (*right*) were recorded from 2 posterior sensor sites (A100/A125). The gray areas highlight the time window for which the mean magnetic field distribution was computed. *Inset*: the geometry of overlapping efflux-influx patterns of the magnetic flux that would arise from 2 symmetrical current sources with the same polarity orientation. The black arrows indicate the direction of the generating current sources, the colored arrows indicate the direction of the magnetic flux leaving (red) and entering (blue) the brain.

Magnetic waveforms and distributions

Figure 2*B* illustrates the grand-average MEG waveforms from two posterior sensor sites (A100, A125). The gray areas between the simple- and discriminative-response waveforms highlight the magnetic analog of the N1 discrimination effect. Downward deflections indicate that the magnetic flux is leaving the head (an *efflux*) and upward deflections indicate that the magnetic flux is entering the head (an *influx*). The magnetic analog of the N1 wave consisted of an efflux over the left hemisphere and an influx over the right hemisphere, and the magnitude of these fluxes was greater for the discriminative-response condition than for the simple-response condition (just as the magnitude of the electrical response was greater for the discriminative-response condition). This is further illustrated in Fig. 3*B*, which shows the time-course and distribution of the mean magnetic field for the discriminative–simple difference waveforms. The gray areas highlight the time range of the early phase of the discrimination effect (140–200 ms), which was the focus of the present analyses. Separate ANOVAs were performed using the data from the left and right posterior sensor sites drawn in white in Fig. 2*B*, with a single factor of condition (simple vs. discriminative response). This ANOVA yielded a significant main effect of condition at both the left- and right-hemisphere sites (*left*: $F(1,9) = 7.64$, $P < 0.05$; *right* $F(1,9) = 6.93$; $P < 0.05$).

In the field distribution map shown in Fig. 3*B*, red lines indicate efflux from the head and blue lines indicate influx into the head. Note that, unlike the ERP voltage maps, the MEG maps show opposite-polarity effects over the left and right hemispheres as would be expected due to the physics of the magnetic signal. More specifically, regions of efflux and influx were present over the left and right occipital lobes, respectively. These regions were separate by a wide transition region—marked with a dashed ellipse—that exhibited very little net flux. This pattern is consistent with the presence of two mirror-symmetrical current sources—each producing an efflux and an influx—that are spatially arranged such that the efflux of one cancels the influx of the other (see Fig. 3*B, inset,* which illustrates the overlapping efflux-influx pattern in a schematic manner). That is, a left occipital current source may produce the efflux observed over the left hemisphere along with a midline influx, and a right occipital current source may produce the influx observed over the right hemisphere along with a midline efflux. The influx and efflux at the midline would then cancel, yielding the observed broad region of little net flux. This would also explain the observation of an efflux over

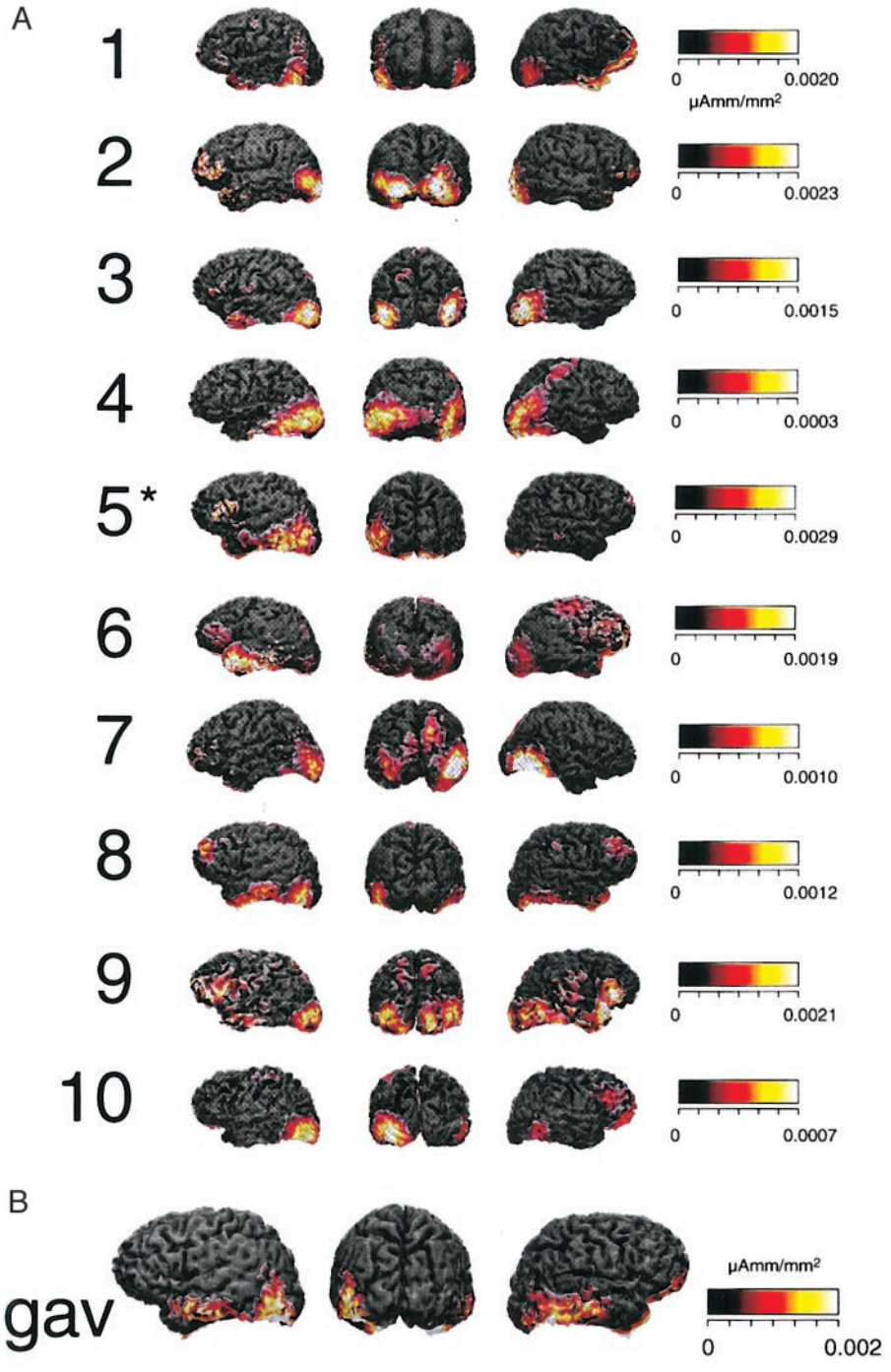

FIG. 4. Distributed-source estimates from the discriminative-simple difference waveforms (EEG and MEG, 140–200 ms) for each individual subject (*A*) and the grand average (*B*) in left-hemisphere, back, and right-hemisphere views. To allow optimal illustration of the source distribution, the plots are scaled differently for each subject.

the left hemisphere and an influx over the right hemisphere, which would be predicted for current sources in these locations that have the same polarity orientation. Note, current sources with the same polarity orientation would be expected for foveal stimulation as has been used in this experiment. This is because visual up-stream projections and their top-down modulatory projections would enter into homologue cortical regions given rough symmetry between hemispheres. Hence, neural currents arising from mirror image cortical regions would also display mirror symmetry compatible with the two negative maxima of the observed electric field (Fig. 3*A*), and the magnetic flux orthogonal to these currents would produce overlapping efflux-influx patterns as illustrated in Fig. 3*B, inset,* consistent with our observed pattern.

Current density estimates

To estimate the cortical distribution of electrical currents that give rise to the magnetic and electric field distributions, the discriminative-simple difference waveforms from both the EEG and MEG recordings were subjected to a compound distributed source analysis (see METHODS).

Figure 4*A* shows distributed-source estimates (140–200 ms) for each subject and the grand average in left-hemisphere,

TABLE 1. *Signal-to-noise ratios in the source reconstruction interval (140–200 ms) of MEG and EEG data for the grand average and the individual subjects*

	SNR		Explained Variance, %	Hemisphere	T&T Coordinates		
	MEG	EEG			*x*	*y*	*z*
GAV	11.7	13.8	98	Left	−50.0	−68.4	−18.5
				Right	56.4	−62.4	−15.1
1	3.9	6.0	94	Left	−61.5	−57.5	−21.2
				Right	32.8	−72.3	−0.1
2	26.6	10.1	98	Left	−36.3	−98.9	−9.2
				Right	26.6	−96.2	−4.6
3	23.8	39.0	99	Left	−52.9	−79.0	−7.5
				Right	32.7	−75.6	−0.5
4	6.8	5.5	89	Left	−53.7	−72.7	−8.9
				Right	37.9	−85.1	−6.9
5	6.3	6.8	97	Left	−47.8	−67.5	−18.7
				Right	33.8	−86.6	−18.6
6	5.4	11.5	89	Left	−59.2	−1.4	−21.9
				Right	32.3	−80.0	−9.2
7	15.7	14.7	98	Left	−44.5	−88.6	−13.9
				Right	53.0	−66.7	−15.2
8	20.1	26.8	99	Left	−51.4	−74.4	−16.1
				Right	40.4	−81.2	−13.2
9	8.2	6.0	94	Left	−42.5	−90.1	−5.9
				Right	53.8	−68.2	−7.3
10	12.3	13.4	95	Left	−50.3	−74.7	−17.1
				Right	58.7	−59.4	−15.7
Centroid				Left	−50.0	−70.5	−14.0
				Right	40.2	−77.1	−9.1

Explained variance indicates the percentage of variance of the measured data that could be explained by the distributed source model based on combined electroencephalographic/magnetoencephalographic (EEG/MEG) data. The three rightmost columns report coordinates of maximum strength for left- and right-hemisphere current sources of the discrimination effect in the coordinate system of Talairach and Tournoux (T&T). SNR, signal-to-noise ratio; GAV, grand average.

back, and right-hemisphere views.[2] Note that the plots are scaled differently for each subject to allow optimal illustration of the source distribution. The grand-average estimates show a strong left inferior occipito-temporal source and a somewhat weaker right inferior occipito-temporal source. For both hemispheres, this activity also spread weakly into more anterior portions of the inferior temporal lobes. The left occipito-temporal source was clearly evident in 9 of the 10 individual subjects (all except *6*), and the right occipito-temporal source tended to be weaker and more variable. The more anterior inferior temporal activity that was evident in the grand average was present in some subjects (e.g., *6* and *8*) but was not clearly present in many other subjects. Some prefrontal activity was also evident in a few of the subjects (e.g., *2, 5,* and *8*).

For each subject, we computed the coordinates of the location with the greatest current density in both the left and right hemispheres, using the reference frame of Talairach and Tournoux (Talairach and Tournoux 1988). These locations are shown in Fig. 5, superimposed on the reconstructed brain of the reference subject. The coordinates are also provided in Table 1, along with information about signal-to-noise ratio and explained variance. These maxima are located in the inferior occipital lobe or occipito-temporal junction for every subject except one (*6*). This high level of consistency indicates that the localization procedure was reasonably accurate and was not substantially distorted by noise. Thus it is reasonable to conclude that the N1 discrimination effect largely reflects activity in inferior occipital or occipito-temporal cortex.

[2] An MR scan was not available for *subject 5,* and the BEM of the reference subject (*8*) was therefore used as an approximation for calculating the distributed source estimates for this subject.

DISCUSSION

The goal of this study was to localize—in both time and space—the effects of top-down control over discriminative processing. As in previous ERP studies (Ritter et al. 1982, 1988; Vogel and Luck 2000), we observed a greater negativity in the ERP waveforms in the time range of the N1 wave for the discriminative-response condition than for the simple-response condition. This effect was largest over occipital cortex, with greater activity over the left hemisphere. This distribution is consistent with previous reports of the N1 discrimination effect. The MEG waveforms also included a larger response in the N1 latency range for the discriminative-response condition than for the simple-response condition, and this effect was again largest at left posterior sites. Thus the intention to perform a discrimination influences both electrical and magnetic responses within 150 ms of stimulus onset.

The timing of the N1 discrimination effect appears to be similar to the timing of the effects of discriminative processing observed by Spitzer and Richmond (1991) in macaque inferotemporal cortex. It is also similar to the timing of some previously observed ERP effects that were related to visual discriminations. For example, Thorpe et al. (1996) recorded ERPs while subjects viewed real-world photographs that either did or did not contain an animal, and they found an enhanced negativity for animal-containing photographs starting around 150 ms poststimulus (see also Fabre-Thorpe et al., 2001). Although

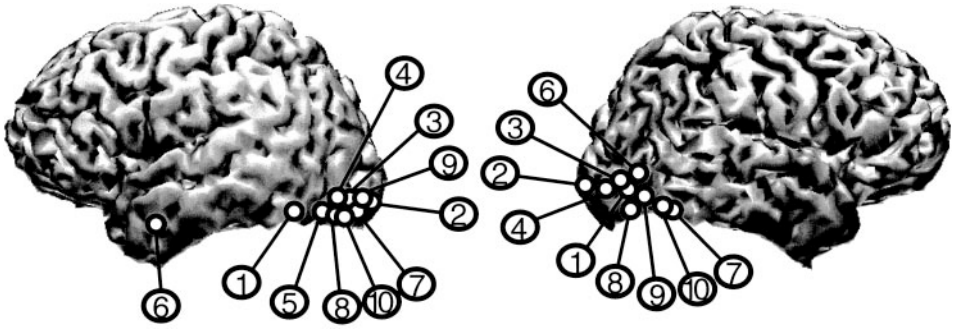

FIG. 5. Locations showing maximum current density in both the left and right hemispheres of each subject (*1–10*). Locations are based on Talairach/Tournoux-coordinates (Talairach and Tournoux 1988) and superimposed on the reconstructed brain of the reference subject.

that effect was largest at frontal electrode sites, the timing was similar to the present N1 discrimination effect. Other studies have also shown that faces and words elicit differential ERP responses compared with other stimuli within 150 ms of stimulus onset (e.g., Bentin et al. 1996; Eimer 1998; Jeffreys 1989; Schendan et al. 1998), and intracranial recordings have yielded similar effects in regions of the posterior fusiform gyrus (Allison et al. 1994). Thus different varieties of complex visual stimuli produce differential activity by 150 ms poststimulus, and the intention to perform a discrimination also produces differential activity in this time range. It therefore seems plausible that the N1 discrimination effect reflects a top-down modulation of stimulus-driven discrimination processes.

The discriminative-response condition was more difficult than the simple-response condition, and it is therefore important to consider whether the observed ERP and MEG effects simply reflect a higher level of arousal. This possibility was addressed experimentally in a previous ERP study (Vogel and Luck 2000) that used nearly identical experimental parameters (stimulus duration, stimulus onset asynchrony (SOA) randomization, instruction for fast and accurate responses; the stimuli, however, were sets of 5 colored letters rather than single-colored squares). In addition to the discriminative- and simple-response conditions used in the present study, the previous study assessed the contribution of arousal by including an additional simple-response condition in which response speed was highly stressed and feedback about RT was given. This speed-stressed condition led to faster RTs and an increase in P1 amplitude, consistent with an increased level of arousal, but the posterior N1 wave was actually reduced in amplitude. Thus increased arousal does not lead to an increased N1 wave.

Although onset latency and source localization suggest that the N1 discrimination effect reflects top-down modulation of sensory processing in the ventral stream, the actual computational function of this modulation remains to be explained. The present findings cannot provide an in-depth answer to this more fundamental question, but we will briefly discuss how the present results are related to a more general modeling framework of top-down cortical processing that has been advanced recently. The predictive coding model (Rao and Ballard 1997, 1999) proposes that top-down-mediated neural responses in the visual cortex mainly reflect the interaction (discrepancy) between the higher levels' predictions about the stimulus features and the actual features registered by bottom-up visual processing. Along these lines, the instruction to discriminate the stimuli in the present study would entail feature (color)-specific predictions to be built up in the cortical regions we have identified, whereas the simple task would not necessitate such predictions. The observed neural activity may reflect the interaction between the bottom-up sensory information and these predictions in the discriminative-response task.

In the present study, the neural generator sources of the N1 discrimination effect were estimated by combining ERP and MEG distributions with structural MR images. There was some variability across subjects in the overall pattern of estimated cortical distributions, but the estimated maximum site of activation was highly similar across both hemispheres and across all subjects except one. This maximum was located in inferior occipital or occipito-temporal cortex, near the border between areas 19 and 37. Previous neuroimaging studies have also shown that active processing of color information leads to enhanced activity in this general region. For example, Corbetta et al. (1990, 1991) compared a passive condition similar to our simple-response condition with focused attention conditions in which subjects performed color, form, and velocity discriminations; an additional divided-attention condition was also included in which subjects performed color, form, and velocity discriminations simultaneously. When the passive condition was subtracted from the attend-color condition, significant activation was observed in the left lingual gyrus. When the divided-attention condition was subtracted from the attend-color condition, a broadband of activation was observed in lateral occipital cortex, particularly in the left hemisphere. The general location and lateralization of these effects are similar to the maximum estimated activity observed in the present study, and they may reflect exactly the same neural processes. Thus the present results suggest that previously observed neuroimaging effects may reflect, in part, activity from approximately 140–200 ms poststimulus.

Spatial attention also influences neural activity in this time range and in this region of cortex. Specifically, attended-location stimuli elicit enhanced N1 waves (e.g., Eimer 1994; Mangun and Hillyard 1990; Van Voorhis and Hillyard 1977), and attended-location stimuli elicit enhanced activity in lateral occipital cortex (e.g., Kastner et al. 1998; Tootell et al. 1998; Woldorff et al. 1997). Moreover, spatial attention does not appear to influence the N1 wave unless subjects perform a discrimination at the attended location (Mangun and Hillyard 1991). Together with the present results, these findings suggest that discriminative processes in human occipital cortex begin to operate within 150 ms poststimulus and are influenced by both the overall intention to perform a discrimination and by spatial attention.

We are grateful to J. Heinrich for technical support and A. Schoenfeld for helpful discussions and comments on earlier versions of the manuscript.

This research was supported by grant RG0136 from the Human Frontier Science Program (G. R. Mangun, principal applicant), grant He1531/3-5 from the Deutsche Forschungs-Gemeinschaft (H.-J. Heinze, principal applicant),

grant MH-56877 from the National Institute of Mental Health (S. J. Luck, principal investigator), and grant SBR 98-09126 from the National Science Foundation (S. J. Luck, principal investigator).

REFERENCES

ALLISON T, MCCARTHY G, NOBRE A, PUCE A, AND BELGER A. Human extrastriate visual cortex and the perception of faces, words, numbers, and colors. *Cereb Cortex* 5: 544–554, 1994.

AMERICAN ELECTRO ENCEPHALOGRAPHIC SOCIETY. Guidline seven: a proposal for standard montages to be used in clinical EEG. *J Clin Neurophysiol* 11: 30–36, 1994.

BENTIN S, MCCARTHY G, PEREZ E, PUCE A, AND ALLISON T. Electrophysiological studies of face perception in humans. *J Cognit Neurosci* 8: 551–565, 1996.

CHAWLA D, REES G, AND FRISTON KJ. The physiological basis of attentional modulation in extrastriate visual areas. *Nat Neurosci* 2: 671–676, 1999.

CLARK VP AND HILLYARD SA. Spatial selective attention affects early extrastriate but not striate components of the visual evoked potential. *J Cognit Neurosci* 8: 387–402, 1996.

CLARK VP, PARASURAMAN R, KEIL K, KULANSKY R, FANNON S, MAISOG JM, UNGERLEIDER LG, AND HAXBY JV. Selective attention to face identity and color studied with fMRI. *Hum Brain Map* 5: 293–297, 1997.

CORBETTA M, MIEZIN FM, DOBMEYER S, SHULMAN GL, AND PETERSEN SE. Attentional modulation of neural processing of shape, color, and velocity in humans. *Science* 248: 1556–1559, 1990.

CORBETTA M, MIEZIN FM, DOBMEYER S, SHULMAN GL, AND PETERSEN SE. Selective and divided attention during visual discriminations of shape, color, and speed: functional anatomy by positron emission tomography. *J Neurosci* 11: 2383–2402, 1991.

DUPONT P, VOGELS R, VANDENBERGHE R, ROSIER A, CORNETTE L, BORMANS G, MORTELMANS L, AND ORBAN GA. Regions in the human brain activated by simultaneous orientation discrimination: a study with positron emission tomography. *Eur J Neurosci* 10: 3689–3699, 1998.

EIMER M. An ERP study on visual spatial priming with peripheral onsets. *Psychophysiology* 31: 154–163, 1994.

EIMER M. Does the face-specific N170 component reflect the activity of a specialized eye processor? *Neuroreport* 9: 2945–2948, 1998.

FABRE-THORPE M, DELORME A, MARLOT C, AND THORPE S. A limit to the speed of processing in ultra-rapid visual categorization of novel natural scenes. *J Cognit Neurosci*13: 171–180, 2001.

FUCHS M, DRENCKHAHN R, WISCHMANN HA, AND WAGNER M. An improved boundary element method for realistic volume-conductor modeling. *IEEE Trans Biomed Eng* 45: 980–997, 1998a.

FUCHS M, WAGNER M, KOHLER T, AND WISCHMANN HA. Linear and nonlinear current density reconstructions. *J Clin Neurophysiol* 16: 267–295, 1999.

FUCHS M, WAGNER M, WISCHMANN HA, KOHLER T, THEISSEN A, DRENCKHAHN R, AND BUCHNER H. Improving source reconstructions by combining bioelectric and biomagnetic data. *Electroencephalogr Clin Neurophysiol* 107: 93–111, 1998b.

GANDHI SP, HEEGER DJ, AND BOYNTON GM. Spatial attention affects brain activity in human primary visual cortex. *Proc Natl Acad Sci USA* 96: 3314–3319, 1999.

HILLYARD SA, VOGEL EK, AND LUCK SJ. Sensory gain control (amplification) as a mechanism of selective attention: electrophysiological and neuroimaging evidence. *Philos Trans R Soc Lond B Biol Sci* 353: 1257–1270, 1998.

ITO M AND GILBERT CD. Attention modulates contextual influences in the primary visual cortex of alert monkeys. *Neuron* 22: 593–604. 1999.

JEFFREYS DA. A face-responsive potential recorded from the human scalp. *Exp Brain Res* 78: 193–202, 1989.

JENNINGS JR AND WOOD CC. The epsilon-adjustment procedure for repeated-measures analyses of variance. *Psychophysiology* 13: 277–278, 1976.

KASTNER S, DE WEERD P, DESIMONE R, AND UNGERLEIDER LG. Mechanisms of directed attention in the human extrastriate cortex as revealed by functional MRI. *Science* 282: 108–111, 1998.

LUCK SJ, CHELAZZI L, HILLYARD SA, AND DESIMONE R. Neural mechanisms of spatial selective attention in areas V1, V2, and V4 of macaque visual cortex. *J Neurophysiol* 77: 24–42, 1997.

LUCK SJ AND HILLYARD SA. The role of attention in feature detection and conjunction discrimination: an electrophysiological analysis. *Intern J Neurosci* 80: 281–297, 1995.

LUCK SJ AND VECERA SP. *Attention: From Paradigms to Mechanisms. Stevens' Handbook of Experimental Psychology. Sensation and Perception,* edited by Yantis S. New York: Wiley, 2002, vol. 1, p. 235–286.

MANGUN GR. Neural mechanisms of visual selective attention. *Psychophysiology* 32: 4–18, 1995.

MANGUN GR AND HILLYARD SA. Allocation of visual attention to spatial location: Event-related brain potentials and detection performance. *Percept Psychophys* 47: 532–550, 1990.

MANGUN GR AND HILLYARD SA. Modulations of sensory-evoked brain potentials indicate changes in perceptual processing during visual-spatial priming. *J Exp Psychol Hum Percept Perform* 17: 1057–1074, 1991.

MANGUN GR, HANSEN JC, AND HILLYARD SA. Electroretinograms reveal no evidence for centrifugal modulation of retinal input during selective attention in man. *Psychophysiology* 23: 156–165, 1986.

MANGUN GR, HOPFINGER JB, KUSSMAUL CL, FLETCHER EM, AND HEINZE H.-J. Covariations in ERP and PET measures of spatial selective attention in human extrastriate visual cortex. *Hum Brain Map* 5: 273–279, 1997.

MARTINEZ A, ANLLO-VENTO L, SERENO MI, FRANK LR, BUXTON RB, DUBOWITZ DJ, WONG EC, HINRICHS H, HEINZE HJ, AND HILLYARD SA. Involvement of striate and extrastriate visual cortical areas in spatial attention. *Nat Neurosci* 2: 364–369, 1999.

MOTTER BC. Focal attention produces spatially selective processing in visual cortical areas V1, V2, and V4 in the presence of competing stimuli. *J Neurophysiol* 70: 909–919, 1993.

RAO RP AND BALLARD DH. Dynamic model of visual recognition predicts neural response properties in the visual cortex. *Neural Comput* 9: 721–763, 1997.

RAO RP AND BALLARD DH. Predictive coding in the visual cortex: a functional interpretation of some extra-classical receptive-field effects. *Nat Neurosci* 2: 79–87, 1999.

RITTER W, SIMSON R, AND VAUGHAN HG. Event-related potential correlates of two stages of information processing in physical and semantic discrimination tasks. *Psychophysiology* 20: 168–179, 1983.

RITTER W, SIMSON R, AND VAUGHAN HG. Effects of the amount of stimulus information processed on negative event-related potentials. *Electroencephalogr Clin Neurophysiol* 69: 244–258, 1988.

RITTER W, SIMSON R, VAUGHAN HG, AND MACHT M. Manipulation of event-related potential manifestations of information processing stages. *Science* 218: 909–911, 1982.

ROBINSON SE. Environmental noise cancellation for biomagnetic measurements. In: *Advances in Biomagnetism,* edited by Williamson SJ, Hoke M, Stroink G, and Kotani M. New York: Plenum, 1989, p. 721–724.

ROELFSEMA PR, LAMME VAF, AND SPEKREIJSE H. Object-based attention in the primary visual cortex of the macaque monkey. *Nature* 395: 376–381, 1998.

SCHENDAN HE, GANIS G, AND KUTAS M. Neurophysiological evidence for visual perceptual categorization of words and faces within 150 ms. *Psychophysiology* 35: 240–251, 1998.

SHULMAN GL, CORBETTA M, BUCKNER RL, RAICHLE ME, FIEZ JA, MIEZIN FM, AND PETERSEN SE. Top-down modulation of early sensory cortex. *Cereb Cortex* 7: 193–206, 1997.

SOMERS DC, DALE AM, SEIFFERT AE, AND TOOTELL RBH. Functional MRI reveals spatially specific attentional modulation in human primary visual cortex. *Proc Natl Acad Sci USA* 96: 1663–1668, 1999.

SPITZER H AND RICHMOND BJ. Task difficulty: ignoring, attending to, and discriminating a visual stimulus yield progressively more activity in inferior temporal neurons. *Exp Brain Res* 83: 340–348, 1991.

TALAIRACH J AND TOURNOUX P. *Co-planar Stereotaxic Atlas of the Human Brain: 3-Dimensional Proportional System: An Approach to Cerebral Imaging*. Stuttgard, Germany: Thieme Verlag, 1988.

THORPE S, FIZE D, AND MARLOT C. Speed of processing in the human visual system. *Nature* 381: 520–522, 1996.

TOOTELL RB, HADJIKHANI N, HALL EK, MARRETT S, VANDUFFEL W, VAUGHAN JT, AND DALE AM. The retinotopy of visual spatial attention. *Neuron* 21: 1409–1422, 1998.

VAN VOORHIS ST AND HILLYARD SA. Visual evoked potentials and selective attention to points in space. *Percept Psychophys* 22: 54–62, 1977.

VOGEL EK AND LUCK SJ. The visual N1 component as an index of a discrimination process. *Psychophysiology* 37: 190–203, 2000.

WOJCIULIK E, KANWISHER N, AND DRIVER J. Covert visual attention modulates face-specific activity in the human fusiform gyrus: fMRI study. *J Neurophysiol* 79: 1574–1578, 1998.

WOLDORFF MG, FOX PT, MATZKE M, LANCASTER JL, VEERASWAMY S, ZAMARRIPA F, SEABOLT M, GLASS T, GAO JH, MARTIN CC, AND JERABEK P. Retinotopic organization of early visual spatial attention effects as revealed by PET and ERPs. *Hum Brain Map* 5: 280–286, 1997.